Article:

Riccobono, Alessio, Parker, Rachel Roberta, Whitwood, Adrian C. et al. (4 more authors) (2018) 1,2,4-Triazolium Ions as Flexible Scaffolds for the Construction of Polyphilic Ionic Liquid Crystals. Chemical Communications. pp. 9965-9968. ISSN 1364-548X

https://doi.org/10.1039/c8cc04704a

ChemComm

Accepted Manuscript

This article can be cited before page numbers have been issued, to do this please use: A. Riccobono, R. R. Parker, A. C. Whitwood, J. M. Slattery, D. W. Bruce, I. PIBIRI and A. Pace, *Chem. Commun.*, 2018, DOI: 10.1039/C8CC04704A.

Volume 52 | Number 1 | 4 January 2016 | Pages 1–216

ChemComm

Chemical Communications
www.rsc.org/chemcomm

ISSN 1359-7345

ROYAL SOCIETY OF CHEMISTRY

COMMUNICATION
Marilyn M. Olmstead, Alan L. Balch, Josep M. Poblet, Luis Echegoyen *et al.*
Reactivity differences of $Sc_3N@C_{2n}$ ($2n$ = 68 and 80). Synthesis of the first methanofullerene derivatives of $Sc_3N@D_{5h}$-C_{80}

175 YEARS

View Article Online
DOI: 10.1039/C8CC04704A

Journal Name

COMMUNICATION

1,2,4-Triazolium Ions as Flexible Scaffolds for the Construction of Polyphilic Ionic Liquid Crystals

Received 00th January 20xx,
Accepted 00th January 20xx

DOI: 10.1039/x0xx00000x

www.rsc.org/

Alessio Riccobono,[a,b] Rachel R. Parker,[b] Adrian C. Whitwood,[b] John M. Slattery,[b]* Duncan W. Bruce,[b] Ivana Pibiri[a]* and Andrea Pace[a]

A novel scaffold for the construction of self-organised ionic liquids and ionic liquid crystals bearing both perfluorocarbon and hydrocarbon moieties has been developed. The phase behaviour and physical properties of these materials can be tuned as a function of chain length and fluorine content and significant structural elaboration is possible, giving a highly flexible system.

Ionic liquid crystals (ILCs) are organic materials combining the low volatility and solvent properties of ionic liquids (ILs) with the intrinsic order and anisotropy of liquid crystals (LCs).[1] They can be exploited as electrolytes for batteries,[2] in electrochemical sensors,[3,4] dye-sensitised solar cells,[5] in water desalination membranes,[6] as solvents in extraction processes,[1] or as media for chemical reactions.[7]

The majority of previous work on ILCs has been based on a limited number of cationic core structures, most commonly imidazolium and pyridinium ions.[1,8] However, the exploration of other core structures is very important, as this is a key variable in the modulation of mesophase behaviour,[9,10] not least because electrostatic interactions between ionic heterocycles and their counterions leads to different types of aggregation.[1]

Also fundamental to the structural chemistry of these systems is the localized organization in which separation of non-polar (most commonly aliphatic chains) and polar (charged) regions can be expected. The complexity and tuneability of the system can then be increased further by inclusion of fluorocarbon chains, which can introduce an additional driving force for self-organisation[11–13] and have tended to promote the formation of lamellar phases[14–16] as well as introducing specific properties such as, for example, gas sorption.[17] Combining these different factors can then give a very significant level of control over both the properties of ionic liquids (ILs) and the phase behaviour of ionic liquid crystals (ILCs).[14,16,18,19]

In this context, we have explored the synthesis, phase behaviour and properties of a new family of polyphilic organic salts containing both perfluorocarbon and hydrocarbon chains at a cationic, aryl triazolium core (Fig. 1). The 1,2,4-triazolium core is a very versatile scaffold for the introduction of further chemical diversity in the design of ILCs and can be prepared with a range of substituents via the robust ANRORC reaction.[18,20–22] This allows variation of the substituents around the heterocyclic core in a modular fashion from a plethora of readily obtained building blocks such as nitriles, fluorinated acids and substituted hydrazines. The choice of the alkylating agent and anion metathesis also introduces further variations on the final structure. This chemical framework has not previously been exploited in ILC chemistry, but provides significant and highly desirable opportunities for structural elaboration.

The properties of the system can be tuned through the interplay of cation-anion interactions, phase separation of aliphatic, fluorocarbon and polar components, and the angular distribution of groups around the heterocyclic core. Triazolium salts have been

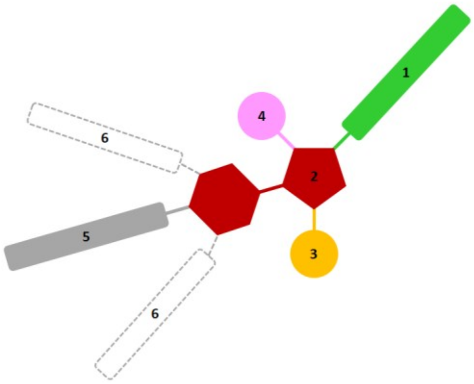

Fig. 1 Schematic representation of the flexible scaffold for cationic aryl triazolium mesogens: **1** = perfluoroalkyl chain; **2** = aryl triazole core; **3** = H, aryl or alkyl; **4** = H or alkyl; **5** = alkyl chain and **6** = optional alkyl chains. This work focusses on salts with CH_3 at points **3** and **4**, as well as perfluoroalkyl chains of different lengths (C_3 and C_7) at point **1** and different alkyl chains (C_{10}, C_{12} and C_{14}) at point **5**.

---

[a] Dipartimento di Scienze e Tecnologie Biologiche, Chimiche e Farmaceutiche, Università degli Studi di Palermo, Via delle Scienze Edificio 17, Palermo, 90128, (Italy).
[b] Department of Chemistry, University of York, Heslington, York, YO10 5DD, (UK

† Footnotes relating to the title and/or authors should appear here.
Electronic Supplementary Information (ESI) available: [details of any supplementary information available should be included here]. See DOI: 10.1039/x0xx00000x

View Article Online
DOI: 10.1039/C8CC04704A

explored in halogen bonding[23], as ILs[24,25] and polyelectrolytes.[26] However, despite their structural analogy with imidazolium ions, there are relatively few reports of LC behaviour for triazolium salts (these involve 1,2,3-substitution).[27–29] While it is generally not possible to form imidazolium salts with perfluorinated chains, herein, we present the first examples of ILCs based on perfluoroalkylated 1,2,4-triazolium salts by direct alkylation of the corresponding 3-perfluoroalkyl-1,2,4-triazoles. These were prepared by ANRORC (*A*ddition of a *N*ucleophile, *R*ing-*O*pening, *R*ing-*C*losure) rearrangements[18,20–22] of 1,2,4-oxadiazole precursors. Thus, 5-perfluoroalkyl-1,2,4-oxadiazoles (**3-*m***) were prepared, *via* the amidoxime route,[30,31] by reaction of 4-methoxybenzamidoxime (**2**) with a perfluoroacyl chloride through dehydrocyclization of an *O*-perfluoroacylamidoxime intermediate. Then, 1,2,4-oxadiazoles **3-m** undergo nucleophilic attack at the C(5) by the less hindered end of methylhydrazine, producing an open-chain intermediate that cyclizes into 1,2,4-triazole **4m** with the loss of hydroxylamine.

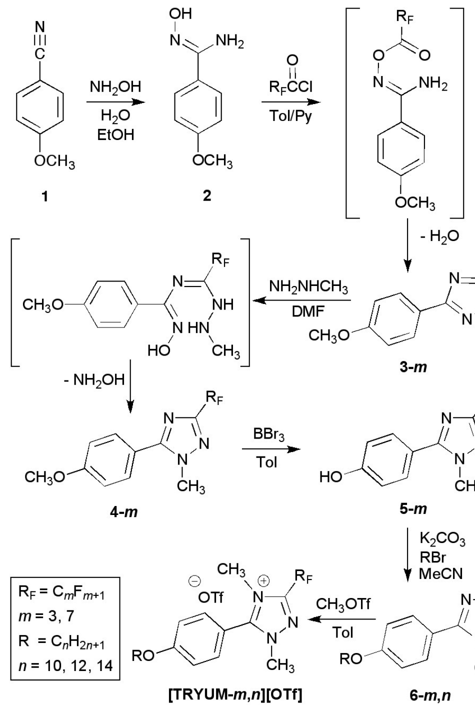

Scheme 1 Synthetic pathway followed to obtain the *N*-methyltriazolium triflates.

Subsequent demethylation with BBr$_3$, and alkylation with long chain alkyl bromides, produced 1,2,4-triazoles **6-*m*,*n*** in good yield and high purity. The latter, were methylated with methyl triflate in toluene or dichloromethane[32–34] yielding final 1,2,4-triazolium salts (**[TRYUM-*m*,*n*][OTf]**) (Scheme 1). The preferred site of methylation for 3,5-disubstituted-1,2,4-triazoles is the more nucleophilic and sterically less hindered *N*(4) position.[35] This was confirmed here by determination of the single-crystal X-ray structure of [TRYUM-7,10][OTf] (Fig. 2). Despite the notional bend angle of *ca* 140° at the heterocycle core, the cation is remarkably linear and the packing motif (Fig. 2b) shows cation-anion alternation with the anions quite closely associated with the triazolium cation. Each triflate is associated with a C(3) of a neighbouring cation through one oxygen and with the C(3)-N(2) bond of another using a different oxygen. Interestingly, such interactions are now referred to as *tetrel bonding* and the former would be regarded as interaction with a σ-hole, while the latter would be with a π-hole.[36,37]

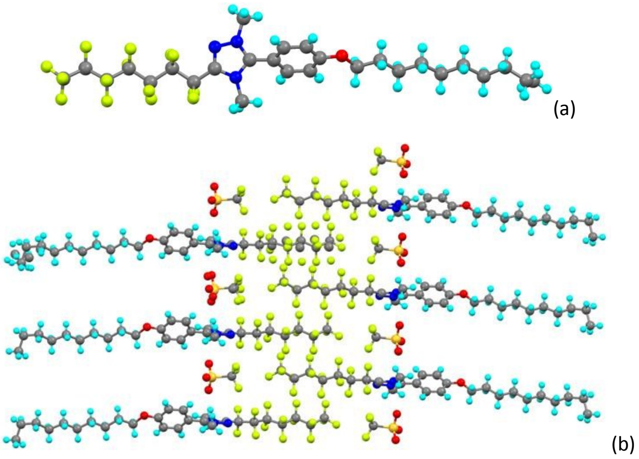

Fig. 2 (a) Structure of the [TRYUM-7,10] cation and (b) the solid-state packing.

The thermal and LC properties of the triazolium triflates were characterised using polarised optical microscopy (POM) and differential scanning calorimetry (DSC) (Table 1).

Table 1. Transition temperatures and enthalpies obtained from the DSC traces.

Compound	Transition	*T* (°C)	Δ*H* (kJ mol^{-1})
[TRYUM-3,10][OTf]	Cr - Cr’	60.0	7.0
	Cr’-Iso	101.5	21.0
[TRYUM-3,12][OTf]	Cr-Iso	91.5	48.5
[TRYUM-3,14][OTf]	Cr-Iso	74.0	38.5
[TRYUM-7,10][OTf]	Cr-SmA	105.5	11.5
	SmA-Iso	161.0	5.0
[TRYUM-7,12][OTf]	Cr-SmA	60.5	36.0
	SmA-Iso	163.5	5.0
[TRYUM-7,14][OTf]	Cr-SmA	52.0	12.0
	SmA-Iso	167.0	5.0

Transitions refer to the 1st heating cycles, while the 2nd heating and 1st cooling are discussed later with the DSC traces.

While none of the neutral precursors **6-*m*,*n*** or the salts with perfluoropropyl-chains was mesomorphic, salts with the longer perfluoroheptyl chains were all ILCs with SmA phases. Fig. 3 shows a representative optical texture for the SmA phases, identified by their focal conic fan texture formed from the coalescence of bâtonnets.[38] A preliminary SAXS study identified *d*-spacings for the 001 reflections of the SmA phases of [TRYUM-7,*n*][OTf] (n = 10, 12 and 14) of 36, 47 and 48 Å respectively. As the length of the alkyl chain increases, the triazolium triflates show an increasing trend of SmA phase stability, which is driven by a modest increase in clearing point with chain length and a rather more marked destabilisation of the crystal phase. The crystal phase is also destabilised with alkyl chain length in the perfluoropropyl salts (Fig. 4). Consistent with observations by POM, DSC studies of **[TRYUM-3,*n*][OTf]** salts show only a Cr-Iso phase transition on heating and crystallisation on cooling. However, for the **[TRYUM-7,*n*][OTf]** salts, the traces showed

View Article Online
DOI: 10.1039/C8CC04704A

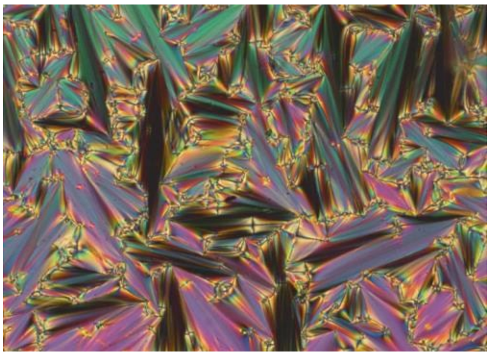

Fig. 3 Photomicrograph of the focal-conic fan texture of the SmA phase **[TRYUM-7,10][OTf]** taken at 160 °C on cooling from the isotropic liquid (100x).

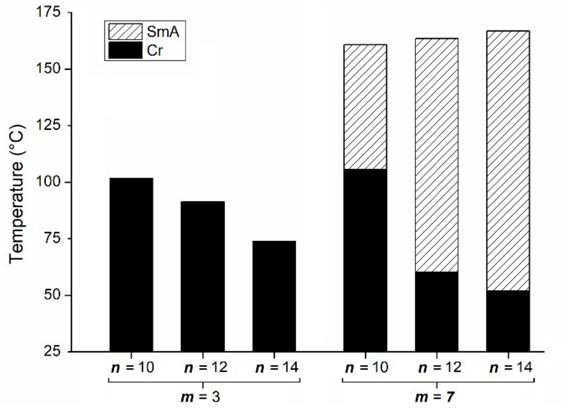

Fig. 4 Bar chart of transition temperatures on 1st heating of the triazolium triflates **[TRYUM-*m,n*][OTf]** grouped by perfluoroalkyl-chain.

slightly more complex behaviour. Thus, on the 1st heating, for *n* = 10, 12 and 14, all salts show a melting point (Cr – SmA) and a clearing point (SmA – Iso) at the temperatures recorded in Table 1. For *n* = 10, cooling then shows a first-order crystallisation at around 60 °C, which is significantly supercooled compared to the melting point of 106 °C (Fig. 5). Its enthalpy is also smaller (–3.5 kJ mol^{-1}) than that of the melting point, implying the existence of more than one crystal phase. **[TRYUM-7,12][OTf]** shows less supercooling of the SmA phase (ΔH for the event at *ca* 30 °C is –11.5 kJ mol^{-1}), but the heating curve appears to show a melting event followed by some recrystallisation, implying that the crystal phase formed on cooling is metastable and reverts to a more stable polymorph following this sequential melting/crystallisation event. This is consistent with the thermal data and the behaviour of **[TRYUM-7,10][OTf]**. The behaviour of **[TRYUM-7,14][OTf]** is straightforward with only a moderate (*ca* 20 °C) supercooling of the SmA – Cr transition. The data show that the clearing points are all but independent of the alkyl chain length, whereas for melting points, that of **[TRYUM-7,10][OTf]** is appreciably higher (106 °C) than those of **[TRYUM-7,12][OTf]** and **[TRYUM-7,14][OTf]**, which are similar to one another (60 and 52 °C, respectively).

Due to the interest in ILs and ILCs as electrolytes,[39] and for the information on ion mobility that it provides, conductivity data for the salts described here were measured using Electrochemical Impedance Spectroscopy (EIS) in a bespoke high-temperature cell.[40–42] Samples were analysed in the LC and/or isotropic phases over a range of temperatures, collecting 4 or 5 points of conductivity/temperature in each phase. Due to the high temperatures used in these measurements, the thermal stability of the triazolium salts was investigated by thermogravimetric analysis (TGA). The onset temperatures for substantial thermal degradation were always over 266 °C, significantly higher than the temperatures used for the EIS measurements. Conductivities were extracted by fitting the EIS data to a suitable equivalent circuit model (see ESI).

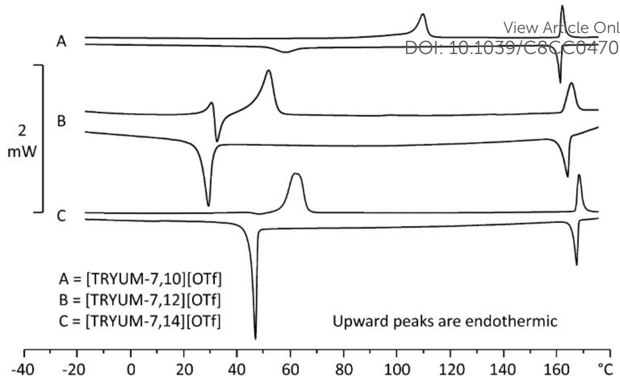

Fig. 5 DSC traces of **[TRYUM-7,*n*][OTf]** showing the 2nd heating and the 1st cooling cycles.

Conductivities increased exponentially with temperature, as expected, and the data fitted well to the Arrhenius model (Fig. 6), although the Vogel-Fulcher-Tamman (VFT) model could be used equally successfully. In ILs, increased conductivities are often found for salts containing ions with the smallest molecular volumes.[43] The picture here is more complex. At the same absolute temperatures the triazolium triflates with C_7F_{15} chains show increasing conductivities with decreasing alkyl chain length, although the SmA phases show only very small differences. Salts with C_3F_7 chains have higher conductivities as the alkyl chain length increases. This may be because **[TRYUM-3,10][OTf]** is close to its melting point at the temperatures where its conductivity can be compared to **[TRYUM-3,14][OTf]**.

The conductivity of **[TRYUM-3,*n*][OTf]** at around 110°C (σ = 50 – 100 × 10^{-6} S cm^{-1}) is in the range of previously observed conductivities for other ILs based on 1,2,3-triazolium salts.[44] It is not possible to directly compare the conductivities between the SmA and isotropic phases, as the isotropic phases are always found at higher temperatures, where conductivity is higher. However, the activation energies (E_a) for ion mobility derived from the Arrhenius fitting (Fig. 6) provide some insight. For both **[TRYUM-7,10][OTf]** and **[TRYUM-7,14][OTf]** E_a is lower for the isotropic phase than for the SmA phase, which suggests reduced ion mobility due to long-range anisotropic ordering in the ILCs.

This work describes the synthesis, phase behaviour and properties of a new family of triazolium-based ILCs. The formation of LC phases in this system requires both alkyl and fluorinated chains to be of a minimum length. Shorter perfluoroalkyl chains (C_3F_7) do not promote mesogenic behaviour, even in the presence of a long $C_{14}H_{29}$ alkyl chain. Whereas with C_7F_{15} chains, SmA phases are observed. Increasing the alkyl chain length reduces the melting points of all salts, but has negligible impact on their clearing points. Thus, the largest mesophase temperature range (115 °C) is seen with

View Article Online
DOI: 10.1039/C8CC04704A

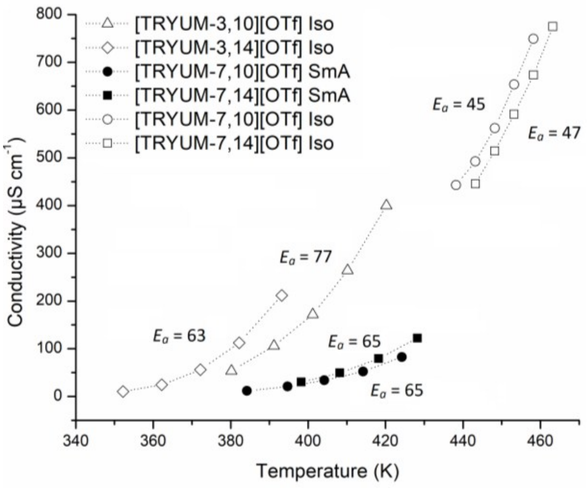

Fig. 6 Plot of triazolium triflate conductivities recorded in SmA and isotropic phases as function of temperature. Dashed lines indicate fits to the data using the Arrhenius model. Activation energies (E_a) from this model are shown in kJ mol^{-1}.

the longest alkyl chain. Conductivities increase exponentially with temperature (Arrhenius or VFT behaviour) and ion mobility is higher in the isotropic liquids compared to the SmA phases. This study focussed on chain length variation, but the novel cation offers many opportunities for further structural elaboration giving access to a family of structurally diverse ILCs.

Notes and references

1 K. Goossens, K. Lava, C. W. Bielawski and K. Binnemans, *Chem. Rev.*, 2016, **116**, 4643–4807.
2 M. Yoshio, T. Kagata, K. Hoshino, T. Mukai, H. Ohno and T. Kato, *J. Am. Chem. Soc.*, 2006, **128**, 5570–5577.
3 A. Safavi and M. Tohidi, *J. Phys. Chem. C.*, 2010, **114**, 6132–6140.
4 N. V. Shvedene, O. A. Avramenko, V. E. Baulin, L. G. Tomilova and I. V. Pletnev, *Electroanalysis*, 2011, **23**, 1067–1072.
5 M. Yoshio, T. Ichikawa, H. Shimura, T. Kagata, A. Hamasaki, T. Mukai, H. Ohno and T. Kato, *Bull. Chem. Soc. Jpn.*, 2007, **80**, 1836–1841.
6 M. Henmi, K. Nakatsuji, T. Ichikawa, H. Tomioka, T. Sakamoto, M. Yoshio and T. Kato, *Adv. Mater.*, 2012, **24**, 2238–2241.
7 D. W. Bruce, Y. Gao, J. N. Canongia Lopes, K. Shimizu and J. M. Slattery, *Chem. - A Eur. JournalA Eur. J.*, 2016, **22**, 16113–16123.
8 K. V. Axenov and S. Laschat, *Materials (Basel).*, 2011, **4**, 206–259.
9 T. J. Dingemans, N. S. Murthy and E. T. Samulski, *J. Phys. Chem. B*, 2001, **105**, 8845–8860.
10 S. I. Torgova, T. A. Geivandova, O. Francescangeli and A. Strigazzi, *Pramana – J. Phys.*, 2003, **61**, 239–248.
11 M. Hird, *Chem. Soc. Rev.*, 2007, **36**, 2070–2095.
12 S. Pensec, F.-G. Tournilhac, P. Bassoul and C. Durliat, *J. Phys. Chem. B*, 1998, **102**, 52–60.
13 C. Tschierske, *Top. Curr. Chem.*, 2011, **318**, 1–108.
14 A. Abate, A. Petrozza, G. Cavallo, G. Lanzani, F. Matteucci, D. W. Bruce, N. Houbenov, P. Metrangolo and G. Resnati, *J. Mater. Chem. A*, 2013, **1**, 6572–6578.
15 I. Zama, G. Gorni, V. Borzatta, M. C. Cassani, C. Crupi and G. Di Marco, *J. Mol. Liq.*, 2016, **223**, 749–753.
16 F. Lo Celso, I. Pibiri, A. Triolo, R. Triolo, A. Pace, S. Buscemi and N. Vivona, *J. Mater. Chem.*, 2007, **17**, 1201–1208.
17 D. Almantariotis, T. Gefflaut, A. A. H. Pádua, J.-Y. Coxam and M. F. C. Gomes, *J. Phys. Chem. B*, 2010, **114**, 3608–3617.
18 I. Pibiri, A. Pace, S. Buscemi, N. Vivona and L. Malpezzi, *Heterocycles*, 2006, **68**, 307–321.
19 I. Pibiri, A. Pace, A. Palumbo Piccionello, P. Pierro and S. Buscemi, *Heterocycles*, 2006, **68**, 2653–2661.
20 S. Buscemi, A. Pace, I. Pibiri, N. Vivona and D. Spinelli, *J. Org. Chem.*, 2003, **68**, 605–608.
21 S. Buscemi, A. Pace, I. Pibiri, N. Vivona, C. Z. Lanza and D. Spinelli, *European J. Org. Chem.*, 2004, **2004**, 974–980.
22 A. Pace, S. Buscemi and N. Vivona, *Org. Prep. Proced. Int.*, 2005, **37**, 447–506.
23 F. Kniep, L. Rout, S. M. Walter, H. K. V. Bensch, S. H. Jungbauer, E. Herdtweck and S. M. Huber, *Chem. Commun.*, 2012, **48**, 9299–9301.
24 S. Sanghi, E. Willett, C. Versek, M. Tuominen and E. B. Coughlin, *RSC Adv.*, 2012, **2**, 848–853.
25 J. M. Aizpurua, R. M. Fratila, Z. Monasterio, N. Pérez-Esnaola, E. Andreieff, A. Irastorza and M. Sagartzazu-Aizpurua, *New J. Chem.*, 2014, **38**, 474–480.
26 M. M. Obadia and E. Drockenmuller, *Chem. Commun.*, 2016, **52**, 2433–2450.
27 K. Stappert, G. Lipinski, G. Kopiec, E. T. Spielberg and A. V. Mudring, *Cryst. Growth Des.*, 2015, **15**, 5388–5396.
28 K. Stappert and A.-V. Mudring, *RSC Adv.*, 2015, **5**, 16886–16896.
29 K. Stappert, D. Uenal, B. Mallick and A. V. Mudring, *J. Mater. Chem. C*, 2014, **2**, 7976–7986.
30 L. B. Clapp, *Adv. Heterocycl. Chem.*, 1976, **20**, 65–116.
31 S. Buscemi, A. Pace, A. P. Piccionello, G. Macaluso, C. Organica, D. Spinelli and G. Giorgi, *J. Mater. Chem.*, 2005, **70**, 3288–3291.
32 R. De Marco, M. L. Di Gioia, A. Liguori, F. Perri, C. Siciliano and M. Spinella, *Tetrahedron*, 2011, **67**, 9708–9714.
33 M. Kajjout, M. Smietana, J. Leroy and C. Rolando, *Tetrahedron Lett.*, 2013, **54**, 1658–1660.
34 T. V. Goncharova, L. V. Zatonskaya and A. S. Potapov, *Procedia Chem.*, 2014, **10**, 485–489.
35 H. Xue, B. Twamley and J. M. Shreeve, *J. Org. Chem.*, 2004, **69**, 1397–1400.
36 A. Bauzá, T. J. Mooibroek and A. Frontera, *ChemPhysChem*, 2015, **16**, 2496–2517.
37 L. Brammer, *Faraday Discuss.*, 2017, **203**, 485–507.
38 J. B. Fournier and G. Durand, *J. Phys. II*, 1991, **1**, 845–870.
39 Y. Wang and H. Yang, *Chem. Eng. J.*, 2009, **147**, 71–78.
40 M. T. Clough, C. R. Crick, J. Gräsvik, P. A. Hunt, H. Niedermeyer, T. Welton and O. P. Whitaker, *Chem. Sci.*, 2015, **6**, 1101–1114.
41 A. J. R. Rennie, V. L. Martins, R. M. Torresi and P. J. Hall, *J. Phys. Chem. C*, 2015, **119**, 23865–23874.
42 J. Katkevics, A. Viksna, A. Zicmanis and G. Vaivars, *Solid State Ionics*, 2011, **188**, 114–117.
43 J. M. Slattery, C. Daguenet, P. J. Dyson, T. J. S. Schubert and I. Krossing, *Angew. Chem. Int. Ed. Engl.*, 2007, **46**, 5384–8.
44 M. M'Sahel, M. M. Obadia, R. Medimagh, A. Serghei, M. Said Zina and E. Drockenmuller, *New J. Chem.*, 2016, **40**, 740–747.

View Article Online
DOI: 10.1039/C8CC04704A